

Received September 6, 2018, accepted October 1, 2018, date of publication October 9, 2018, date of current version November 19, 2018.

Digital Object Identifier 10.1109/ACCESS.2018.2875063

Quantifying Harmonic Responsibilities Based on Kurtosis Detection Principle of Amplitude Fluctuations

JIAN WU¹, HAIFENG QIU^{ID}², (Student Member, IEEE), JINLONG XU¹, FEI ZHOU¹, KANG DAI¹, CHEN YANG¹, AND DONG LV¹

¹State Grid Suzhou Power Supply Company, Suzhou 215004, China

²School of Electrical Engineering, Southeast University, Nanjing 210096, China

Corresponding author: Haifeng Qiu (895416086@qq.com)

This work was supported by the State Grid Corporation of China Science and Technology Project (ADN Comprehensive Demonstration Project of Smart Grid Application Demonstration Area in Suzhou Industrial Park).

ABSTRACT Harmonics have brought non-negligible harm to the safe and stable operation of power systems. In order to quantify the harmonic responsibilities of different stakeholders based on available monitoring data; this paper proposes a novel method based on the kurtosis detection principle of harmonic amplitude fluctuations. The amplitude fluctuation model between the harmonic voltage and current is first established at the point of common coupling, transforming traditional fluctuation method into the amplitude field. Then, the kurtosis detection and interval estimation approaches are adopted to extract the effective fluctuation subsequences of harmonic amplitude data. Finally, the equivalent harmonic impedance of the utility side is calculated to determine the harmonic responsibilities of the utility and customer sides. Simulation and field analysis indicates that the proposed method has higher accuracy on quantifying harmonic responsibilities than the existing methods, and this method avoids the using of harmonic phase-angle data, which can be effectively applied to the practical engineering.

INDEX TERMS Power quality, harmonic responsibilities quantification, harmonic fluctuations, kurtosis detection.

I. INTRODUCTION

With the rapid development of smart grid, various non-linear loads have been connected to power systems in large scale, which has resulted in serious harmonic current injections [1], [2]. The harmonic current flows through the harmonic impedance of the system and forms the harmonic voltage at the point of common coupling (PCC), which leads to the waveform distortions of the supply voltage at the PCC. Thus, it will further affect the operation of other devices at the same bus. For example, harmonics will increase the power loss and reduce the service life of the generators, transmission lines, transformers, and loads. Sometimes, it will also lead to the abnormal operations and faults in devices, even the harmonic resonance phenomenon. Actually, harmonics have quickly spread to the entire network from the local harmonic sources, and brought non-negligible harm to the safe and stable operation of power systems. However, the modern demands on power quality (PQ) are gradually improved, thus

the harmonic problems have severely reduced the economic benefits of the customers [3].

To effectively suppress the harmonics in the grid, the evaluation of harmonic pollutions should be conducted to achieve the sharing of harmonic responsibilities. It is conducive to formulating the incentive rewarding or punishing mechanism according to the harmonic responsibilities of each subject, which encourages and promotes the control of harmonic pollution. While the premise of realizing this mechanism is to accurately quantify the responsibilities of harmonic pollutions caused by different harmonic sources [4]. At present, the research on the quantification of harmonic responsibilities is attributed to the estimation of harmonic impedance [5], [6]. Two methods are mainly used, namely, invasive method and non-invasive method [7]. Invasive method calculates the harmonic impedance through injecting harmonic currents to the system or opening a branch off [8], [9], but it is easy to cause adverse effects on the operation of the system, thus,

invasive method is limited in the practical application. While non-invasive method uses the measurable harmonic voltage and current at the PCC to estimate the harmonic impedance based on the equivalent circuit. Since non-invasive method directly adopts the measured harmonic data without changing the operating state of power systems, it has become the main research direction in the field of quantifying harmonic responsibilities [10].

Non-invasive method mainly includes linear regression method and fluctuation method. Linear regression method estimates the harmonic impedance based on the linear equation model of the harmonic voltage and current at the PCC. Reference [11] presents a bilinear regression model in which the harmonic voltage and current vectors at the PCC are split into the real and imaginary parts to construct two linear regression equations, the least squares regression is used to calculate the coefficients of the regression equations, i.e. the harmonic impedance. However, this model cannot obtain the resistance component of the harmonic impedance, and it also requires a high consistency of the statistical harmonic data. Considering the measurement errors in the absolute values of the harmonic phase and the unfixed referring phase, Zebardast and Mokhtari [12] put forward replacing the absolute phase with the difference phases between the harmonic voltage and current in the regression equation, which has reduced the adverse effect from the reference point phase-angle variations on the computation of the harmonic impedance. Moreover, in order to determine the responsibilities of each harmonic source in the system with multiple harmonic sources, a distributed K-means clustering method is proposed to realize the harmonic data classification [13], then a bayesian partial least squares regression method is conducted to solve the regression equation considering the influence of the background harmonic fluctuations, which has improved the computational accuracy. Similarly, Zebardast and Mokhtari [14] take into account the effects of the background harmonic fluctuations, and propose a three-point data selection method to properly choose the measured data, then a novel constrained recursive least squares regression method with time-varying forgetting factors is used to calculate the harmonic impedance, which has reduced the harmonic impedance computation errors.

In linear regression method, the system harmonic impedance and background harmonic are regarded as the regression coefficients to be solved. If the regression coefficients are stable, linear regression method has high accuracy. However, the background harmonic fluctuates in the actual system, which results in the calculation errors of the model. In addition, the least squares estimation is adopted to address the complex regression calculation problem. Iterative computation is needed when abnormal harmonic monitoring data exists, and the computational complexity will be significantly increased [15].

To fill the gaps in linear regression method, another non-invasive method, i.e. fluctuation method, has been proposed to determine the harmonic impedance by calculating the

ratio between the harmonic voltage and current fluctuations at the PCC [16]. A traditional fluctuation method is firstly presented in [17], this method assumes that the harmonic voltage fluctuations of the PCC are caused by the harmonic current fluctuations in the customer side, and the plus and minus ratios of the harmonic fluctuations respectively denote the utility and customer harmonic impedances, but the influence of the harmonic current fluctuations in the utility side is neglected. Gong *et al.* [18] firstly use the Nair detection method to extract the harmonic current data with large fluctuations, and then calculate the harmonic impedance by the traditional fluctuation method. Although it has reduced the calculation errors, the synchronous fluctuations of the harmonic voltage and current are not considered, and the Nair coefficient is also difficult to be determined. In [19], a novel FastICA method is proposed to filter and separate the harmonic fluctuation data, the ICA method is actually an effective blind source separation technique based on the independence or weak-correlation of signals. The calculation of the harmonic impedance based on the FastICA has reduced the influence of unstable harmonics in the utility side.

The above methods concentrate on the vector data of harmonics, but the harmonic monitoring system in smart grids always cannot directly get the harmonic phase data. Therefore, Xu *et al.* substitute the amplitude data of the harmonic voltage and current at the PCC into the linear regression equation to avoid the measurement of the harmonic phase [20], but the background harmonics and the harmonic phase are varied in a long detecting time period, thus the calculation error of the harmonic impedance is relatively large. Considering the value of X/R is stable in a power-supply system, the unknown harmonic phase is estimated according to the X/R [21], it has improved the precision of the method in [20] to a certain extent, but there will be some errors between the real and estimated harmonic phase because the obtainable X/R is an experience value, instead of the actual operating value, thus affecting the computational results of the harmonic responsibilities. Reference [22] uses the R-squared statistic to demonstrate the fitting degree of the harmonic voltage and current, a non-parametric regression model is implemented to simulate the background harmonic fluctuations and improve the calculation accuracy of the harmonic impedance. When the background harmonics fluctuate violently, the method still has high errors.

There have been some studies on the harmonic responsibility quantification based on linear regression method without using the harmonic phase-angle information, but linear regression method usually has significant computational errors and complexity. Thus, this paper aims at developing a more proper method based on fluctuation method. The basis of fluctuation method is to extract the fluctuation information. Up till now, anomaly detection algorithms have been effective approaches to solve this problem. Reference [23] points that traditional anomaly detection algorithms based on the pattern density of a series focus on the Gaussian signals of the second order statistics. While for non-Gaussian signals,

the second order statistics are just one part of the information, and it becomes powerless for identifying non-Gaussian signals [24]. Thus, an anomaly detection algorithm with the kurtosis of the higher order statistics is often used to detect a status change in the stochastic process [25]. This paper considers using the kurtosis to detect the violent fluctuations of the harmonic voltage and current. The harmonic always exists in power systems, however, it is relatively stable under normal operating conditions. At this time, the kurtosis of the harmonic data is small. When some harmonic sources startup and shut down, the harmonic will appear rapid and step fluctuations, and the kurtosis detection can be adopted to extract such fluctuations for the harmonic responsibility division.

In this paper, a novel method for the harmonic responsibility quantification is proposed based on the kurtosis detection principle of the amplitude harmonic fluctuations. Kurtosis detection calculates the kurtosis of the harmonic voltage and current amplitude sequences by sliding windows, and these sub-sequences with dominant fluctuations of the customer harmonic current and synchronous fluctuations of the PCC harmonic voltage are selected using the interval estimation. The ratio of the two amplitude fluctuations is determined as the utility equivalent harmonic impedance, and the harmonic responsibility quantification can be finally realized. Simulation and field measurement studies show that the proposed method is more accurate than the existing methods, and it is easy to be applied in engineering.

The remainder of the paper is organized as follows: Section II introduces the amplitude fluctuation model. In Section III, the kurtosis detection principle is presented. Simulation and field measurement studies are discussed in Section IV and V for assessing the proposed method, and Section VI concludes the study of this paper.

II. AMPLITUDE FLUCTUATION MODEL

If the harmonic monitoring device is set up at the PCC, the two sides of the PCC can be equivalent to the utility side and the customer side, the Norton equivalent circuit is shown in Fig. 1(a). The whole network is divided into two sides with the PCC as the demarcation, actually, the loads, electric power transmissions and power electronic equipment exist in both sides at the same time, therefore, the harmonic responsibilities needs to be divided to determine the contributions of the harmonic sources in each side. The equation between the vectors of the harmonic voltage and current at the PCC is:

$$\dot{U}_{PCC} = \dot{U}_S + \dot{I}_{PCC} \cdot Z_S \quad (1)$$

where \dot{U}_{PCC} and \dot{I}_{PCC} represent the vector of the harmonic voltage and current at the PCC, respectively. \dot{U}_S is the vector of the harmonic voltage source of the utility side. Z_S denotes the harmonic impedance of the utility side.

The harmonic responsibilities of the utility and customer sides can be analyzed by the superposition theorem, as shown in Fig. 1(b). \dot{U}_{PCC} denotes the sum of the harmonic contributions of the utility and customer sides. The harmonic

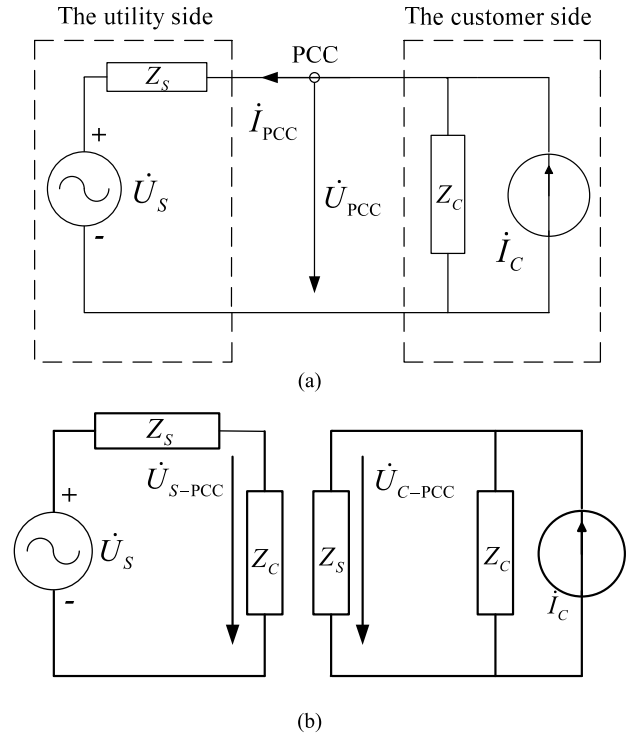


FIGURE 1. Harmonic equivalent circuit. (a) Norton equivalent circuit, (b) Superposition theorem for equivalent circuit.

contributions of each side to \dot{U}_{PCC} are:

$$\begin{cases} \dot{U}_{S-PCC} = \frac{Z_C}{Z_S + Z_C} \cdot \dot{U}_S \\ \dot{U}_{C-PCC} = \frac{Z_S \cdot Z_C}{Z_S + Z_C} \cdot \dot{I}_C \\ \dot{U}_{PCC} = \dot{U}_{S-PCC} + \dot{U}_{C-PCC} \end{cases} \quad (2)$$

where \dot{U}_{C-PCC} and \dot{U}_{S-PCC} respectively illustrate the harmonic contributions of the utility side and the customer side to \dot{U}_{PCC} , Z_C and \dot{I}_C denote the harmonic impedance and the harmonic current of the customer side. \dot{U}_{C-PCC} can be expressed as:

$$\dot{U}_{C-PCC} = \dot{U}_{PCC} - \frac{1}{Z_S/Z_C + 1} \cdot \dot{U}_S \quad (3)$$

Since $Z_C \gg Z_S$ in the system, equation (3) can be rewritten as:

$$\dot{U}_{C-PCC} = \dot{U}_{PCC} - \dot{U}_S \quad (4)$$

The contributions of the utility and customer sides to \dot{U}_{PCC} are determined by the superposition theorem:

$$\begin{cases} \dot{U}_{C-PCC} = \dot{I}_{PCC} \cdot Z_S \\ \dot{U}_{S-PCC} = \dot{U}_S \\ \dot{U}_{PCC} = \dot{U}_{S-PCC} + \dot{U}_{C-PCC} \end{cases} \quad (5)$$

The relations of the vectors in equation (5) are shown in Fig. 2(a). The harmonic voltage responsibilities of the two sides are defined as the ratio of the projections of \dot{U}_{C-PCC} and \dot{U}_{S-PCC} on \dot{U}_{PCC} to the amplitude of \dot{U}_{PCC} . Therefore, the

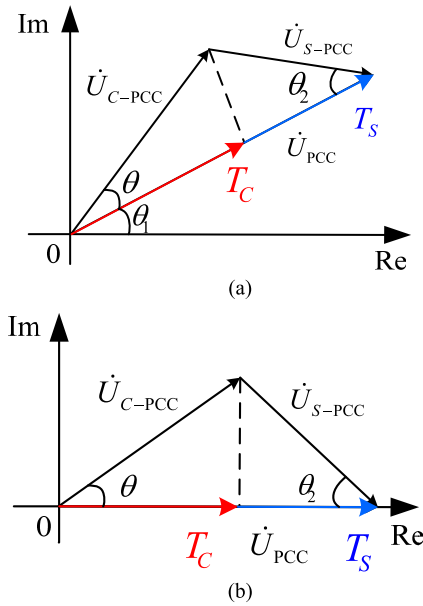


FIGURE 2. Vector diagram of harmonic voltages. (a) Before rotating. (b) After rotating.

harmonic voltage responsibilities of the utility and customer sides are:

$$\begin{cases} T_C = \frac{I_{PCC} |Z_S| \cos \theta}{U_{PCC}} \\ T_S = \frac{U_S \cos \theta_2}{U_{PCC}} \\ T_C + T_S = 1 \end{cases} \quad (6)$$

where T_C and T_S respectively represent the harmonic voltage responsibilities of the utility side and the customer side, and U_{PCC} and I_{PCC} denote the measured amplitudes of \dot{U}_{PCC} and \dot{I}_{PCC} , U_S is the amplitude of \dot{U}_S . θ_1 is the phase angle of \dot{U}_{PCC} , θ_2 indicates the phase angle between \dot{U}_S and \dot{U}_{PCC} , and θ is the phase angle between \dot{U}_{C-PCC} and \dot{U}_{PCC} . In this paper, the vector data refers to the harmonic data containing the amplitude and phase angle information, while the amplitude data represents the amplitude part of the vector data.

The phase-angle of harmonic cannot be obtained accurately in practice, thus it is really difficult to calculate T_C and T_S without the phase-angle data. But, equation (6) shows that the calculation of the harmonic voltage responsibilities is irrelevant to θ_1 , thus \dot{U}_{PCC} is rotated to the positive axis, as shown in Fig. 2(b). The real part of equation (1) is described as:

$$U_{PCC} = U_S \cos \theta_2 + I_{PCC} \cdot |Z_S| \cos \theta \quad (7)$$

The utility harmonic impedance is related to the operation mode and the network topology of the system, it can be regarded as a constant in a short monitoring time period, moreover, the background harmonic is also relatively stable in a short time period. Thus, $|Z_S| \cos \theta$ and $U_S \cos \theta_2$ can be considered as the coefficients of equation (7), and the fluctuations of U_{PCC} are caused by the change of I_{PCC} . If there

is a ΔI_{PCC} in the system, equation (7) can be expressed as:

$$(U_{PCC} + \Delta U_{PCC}) = U_S \cos \theta_2 + (I_{PCC} + \Delta I_{PCC}) \cdot |Z_S| \cos \theta \quad (8)$$

where ΔU_{PCC} and ΔI_{PCC} respectively represent the amplitude fluctuations of the harmonic voltage and harmonic current at PCC, $|Z_S| \cos \theta$ is the equivalent harmonic impedance in the utility side. Subtracting equation (7) from equation (8), the equation is written as:

$$\Delta U_{PCC} = \Delta I_{PCC} \cdot |Z_S| \cos \theta \quad (9)$$

If ΔU_{PCC} and ΔI_{PCC} are detected, we can determine $|Z_S| \cos \theta$ by equation (9), T_C can be calculated according to equation (6).

III. KURTOSIS DETECTION PRINCIPLE OF FLUCTUATIONS

The premise of using equation (9) is that the harmonic voltage and current fluctuations are significant and synchronous, and the background harmonic is relatively stable under these circumstances. Here, significant indicates that the harmonic voltage or current has obvious fluctuations, and it expresses numerically as the variance of the harmonic data is larger than its expected value. Synchronous means that if the harmonic current fluctuates in a short monitoring time period, the similar or opposite fluctuating trend of the harmonic voltage exhibits. Stable demonstrates the background harmonic can be treated as a constant because the operating condition of the system is steady in a short monitoring time period. Therefore we need to select the harmonic data which meets these requirements. The selected harmonic fluctuations in the monitoring data will manifest a large increase or a step change, which is characterized as the significant and rapid change of the harmonic amplitude in one window length, even a step peak or valley. Thus the kurtosis detection method can be used to filter the harmonic fluctuation data.

Kurtosis is a statistic that describes the steepness of a statistical distribution. The kurtosis of a normal distribution is usually normalized to zero. Thus, the data deviating far from the normal distribution produces large kurtosis values. Literature [26] indicates that an impulse series results in heavier tails and a sharper peak of the distribution of the signal's amplitude compared with the Gaussian distribution, leading to an increase in kurtosis value. A high kurtosis means that the increase of the variance is caused by some extreme and low-frequency data which is greater or smaller than the average value. Under normal operating conditions, the harmonic sources in the system are relatively stable. In a short window of several minutes, the harmonic fluctuates around its average value, and there is no extreme data. Although the data may not completely satisfy the normal distribution, the deviating degree is not too large, thus there will be no high kurtosis. However, when the harmonic amplitude has a step or impulse fluctuation, the kurtosis will be much higher than 0.

In order to show the characteristics, we use two groups of the harmonic current data to conduct the testing of the

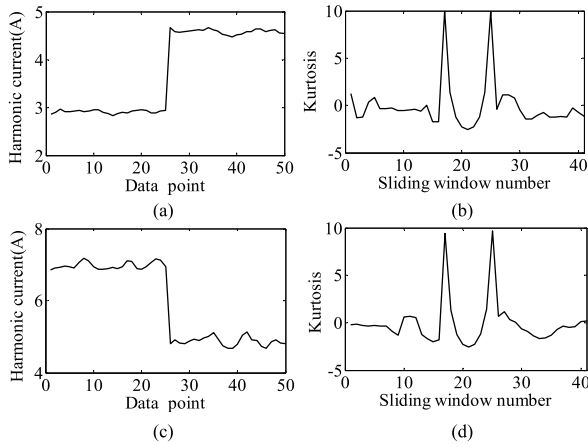


FIGURE 3. Step data and kurtosis. (a) Upper step data, (b) Kurtosis of upper step, (c) Lower step data, (d) Kurtosis of lower step.

upper and lower step kurtosis detections. Each group has 50 data, and produces an obvious step in the 25th data. The sliding distance and the window length are set to be 1 and 10, respectively. Setting the sliding distance to 1 means that all series can be detected step by step. If the sliding distance is larger, some series will be lost. The window length defines the time length and the amount of the data in each kurtosis calculation. From the aspect of time length, it is necessary to ensure that the background harmonic in a window length is relatively stable, thus the window length cannot be too large. Generally, it can be several minutes in an actual engineering system. From the perspective of data amount, one window length should cover enough sampled data. Since the time-interval of actual harmonic monitoring system is several seconds, it is more appropriate to include dozens of sets of data in one window length. At this time, both the time length and the amount of the data in one window are satisfied. In this paper, the window mainly refers to a time window of a few minutes, it is used to define the harmonic data for each kurtosis calculation. The step data and the calculated kurtosis are shown in Fig. 3.

As shown in Fig. 3, the values of the kurtosis fluctuate in the vicinity of zero before the sliding window entering the step point 25, when the right side of the sliding window is the step point, the kurtosis has a high peak, then the kurtosis decreases. When the left side of the sliding window is the step point, the kurtosis also has a high peak. If the sliding window leaves the step point, the kurtosis returned to the normal value around zero.

For a series of $x = \{x(n) : n = 1, 2, \dots, N\}$, the kurtosis can be calculated through the unbiased estimation G , the calculating formula of G is [24]:

$$G = \frac{N \cdot (N + 1) \cdot \sum_{n=1}^N (x(n) - \hat{m})^4}{(N - 1) \cdot (N - 2) \cdot (N - 3) \cdot (\hat{\sigma})^4} - \frac{3 \cdot (N - 1)^2}{(N - 2) \cdot (N - 3)} \quad (10)$$

where \hat{m} and $\hat{\sigma}$ denote the mean and the standard deviation of $x(n)$ respectively.

The kurtosis value K_u is determined using the interval estimate of the normal distribution [27]:

$$K_u = \begin{cases} E(G), & \{E(G) - \frac{\sqrt{\text{var}(G)}}{\sqrt{1-q}} < G < E(G) + \frac{\sqrt{\text{var}(G)}}{\sqrt{1-q}}\} \\ G, & \{-\infty < G \leq E(G) - \frac{\sqrt{\text{var}(G)}}{\sqrt{1-q}}, \\ & E(G) + \frac{\sqrt{\text{var}(G)}}{\sqrt{1-q}} \leq G < +\infty\} \end{cases} \quad (11)$$

where $E(G)$ is the expected value of G , $\text{var}(G)$ represents the variance of G , and q is the confidence interval. The above parameter values are:

$$\begin{cases} E(G) = \frac{-6}{N - 1} \\ \text{var}(G) = \frac{24 \cdot N \cdot (N - 1)^2}{(N - 3) \cdot (N - 2) \cdot (N + 3) \cdot (N + 5)} \\ q = 0.95 \end{cases} \quad (12)$$

The key of the kurtosis detection method is to select these sub-sequences of the harmonic voltage and current with high kurtosis. At this time, the harmonic voltage fluctuations at the PCC are dominated by the fluctuations of the harmonic current. The specific steps of the kurtosis detection method are as follows:

- 1) Collect U_{PCC} and I_{PCC} in the whole concerned time period.
- 2) Set the length of the sliding window W to be L . For practical engineering, L is generally not more than 10 min, a large L may bring difficulties to the kurtosis detection.
- 3) Start with the first data, use equation (10) to calculate the G_U of U_{PCC} and the G_I of I_{PCC} in one W .
- 4) Determine the kurtosis K_{u-U} of U_{PCC} and the kurtosis K_{u-I} of I_{PCC} in one W by equations (11)-(12).
- 5) W moves a point backwards, repeat step 3) and step 4) until W covers the entire time period.
- 6) Select the sub-sequences with $K_{u-U} \neq E(G)$ and $K_{u-I} \neq E(G)$, calculate the equivalent harmonic impedance $|Z_S| \cos \theta$, the average value of $|Z_S| \cos \theta$ is the equivalent harmonic impedance of the concerned time period, use equation (6) to determine the harmonic voltage responsibilities for the customer side.

The proposed method is carried out based on the collected harmonic amplitude data in actual project. Therefore, the errors of this method mainly come from the following aspects: 1) whether the collected harmonic data is accurate. Abnormal data will affect the kurtosis calculation, which further influences the results of harmonic responsibility analysis; 2) whether the window length is reasonable. Large or small L will destroy the calculation effect of the proposed model, thus a proper L should be chosen according to the actual engineering; 3) whether the upstream system is in a stable operating state during an L time period. If the operating mode of the upstream system changes (such as transformer

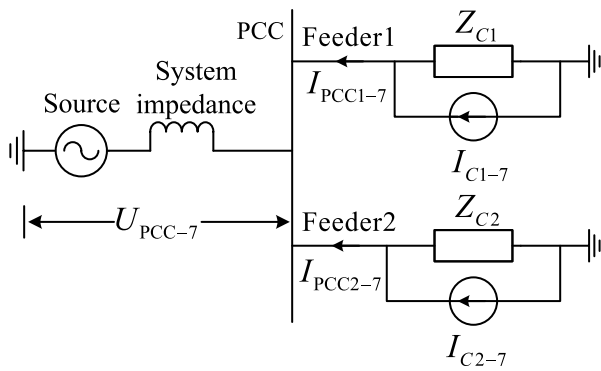


FIGURE 4. Simulation circuit.

operational switching), the equivalent harmonic impedance will also fluctuates, which will have a bad impact on the method. In actual application, the harmonic analysis under different operating modes can be conducted respectively.

This paper mainly analyzes the PQ problem of harmonics. Actually, there are also some other PQ events in the modern smart grid, such as the short flicker, voltage deviation, voltage sag, etc. In engineering, the waveforms of the PQ events are collected and processed firstly, then the series data is use to describe the features of these PQ events. Actually, the proposed model is an effective method for feature extraction and analysis of series data, thus the proposed model can be extended to analyze the characteristics of different PQ problems.

IV. SIMULATION STUDIES

The simulation circuit is shown in Fig. 4, and the model is established in MATLAB. The parameters are set as follows: the system supply voltage $U_N = 10\text{kV}$; the short-circuit capacity $S_k = 100\text{MVA}$; the fundamental impedance of the load in feeder 1 $Z_{C1} = (100 + j314)\Omega$; the fundamental impedance of the load in feeder 2 $Z_{C2} = (150 + j376.8)\Omega$; 7th harmonic current sources are connected to feeder 1 and 2 to simulate the harmonic fluctuations of loads in practical engineering, the amplitude and phase of the 7th harmonic current source of the load in feeder 1 I_{C1-7} fluctuate randomly within $2.7\text{A} \sim 5.4\text{A}$ and $-12^\circ \sim -8^\circ$ respectively. Similarly, the amplitude and phase of I_{C2-7} vary randomly within $4.5\text{A} \sim 7.5\text{A}$ and $-17^\circ \sim -13^\circ$ respectively.

We hope to carry out the simulation research on a system which is similar to the actual engineering. Since this paper mainly discusses the harmonic responsibility division at the 10kV bus and its feeders in a substation, the values of the supply voltage, the short-circuit capacity and the harmonic current sources are set according the national standard of China [28]. In addition, the load impedance parameters are chosen by referring to [5] to ensure $Z_C \gg Z_S$.

Each 0.02s takes one set of amplitude data of the harmonic voltage and current as the samples, the simulation time is 40s, thus a total of 2000 sets of sample data are collected. In order to obtain the 7th harmonic voltage responsibility of feeder 2,

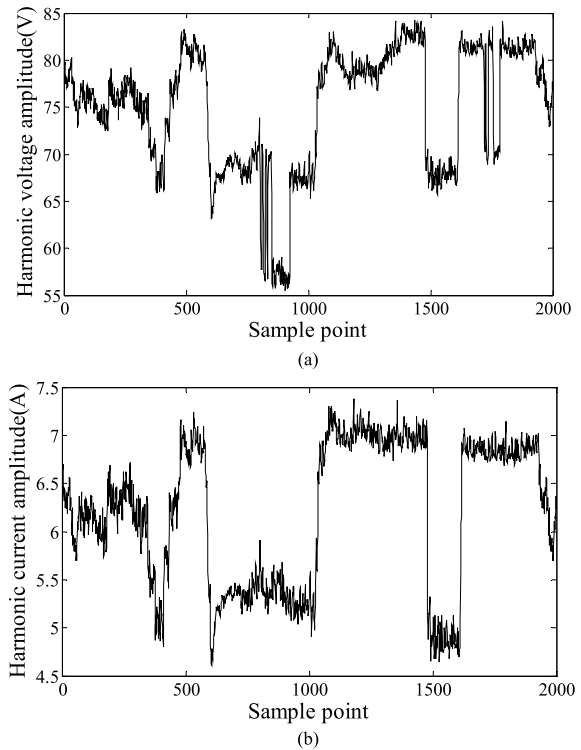


FIGURE 5. Waveforms of sample data. (a) The 7th harmonic voltage amplitude at PCC, (b) The 7th harmonic current amplitude of feeder 2.

TABLE 1. Results of utility equivalent harmonic impedance.

Method	$ Z_s \cos \theta$ (Ω)	Deviations(%)
Exact value	6.90	/
Method1	5.65	-18.12
Method2	7.59	10.00
Proposed method	6.82	-1.16

the 7th harmonic voltage amplitude U_{PCC-7} at the PCC and the 7th harmonic current amplitude I_{PCC2-7} of feeder 2 are measured, the sample data is shown in Fig. 5. To verify the validity and accuracy of the proposed method, three methods are carried out in data analysis to calculate the 7th harmonic voltage responsibility of feeder 2. The errors of different methods are tested by comparing the results with the accurate value.

I_{C2-7} is set to be 0, the harmonic voltage at the PCC is caused by feeder 1, $|Z_s| \cos \theta$ of feeder 2 can be determined, thus the exact 7th harmonic voltage responsibility of feeder 2 is calculated accordingly. In the proposed method, the length of W is set to be 0.4s, 1981 sets of K_{u-U} and K_{u-I} are obtained, the results of kurtosis detection are shown in Fig. 6. 14 sets of sub-sequences are selected with $K_{u-U} \neq E(G)$ and $K_{u-I} \neq E(G)$. The equivalent harmonic impedance and the harmonic voltage responsibility are calculated respectively according to equation (9) and equation (6). All the results of the equivalent harmonic impedance are shown in Table 1.

For $U_N = 10\text{kV}$ and $S_k = 100\text{MVA}$, the system 7th harmonic impedance is 7Ω . Due to the existence of

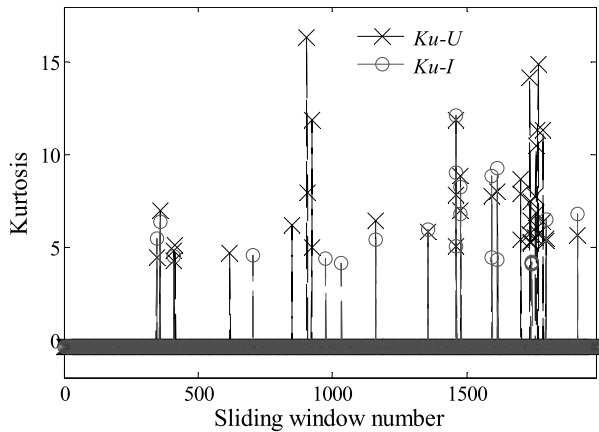


FIGURE 6. Calculation results of kurtosis detection.

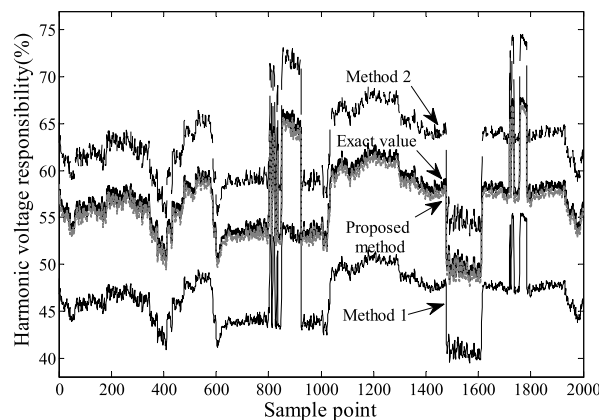


FIGURE 7. Results of harmonic responsibility partition.

TABLE 2. Results and errors of harmonic responsibility.

Method	T_c (%)	Errors(%)
Exact value	57.012	/
Method1	46.691	18.10
Method2	62.723	10.02
Proposed method	56.360	1.14

a small degree $\theta = 5.8^\circ$, the exact equivalent harmonic impedance is 6.9Ω , slightly smaller than 7Ω . Method 1 [21] estimates that θ is 36.18° using the superposition coefficient, θ is too large compared to the actual value, so the equivalent harmonic impedance got from method 1 is smaller than its exact value, with a deviation of -18.12% . The harmonic voltage and current at the 800 and 1700 sampling points in Fig. 6 do not appear a liner correlation, which increases the calculation error of method 2 [22]. The equivalent harmonic impedance calculated by the proposed method has the minimum deviation (-1.16%) in the three methods. The results of harmonic voltage responsibilities are shown in Fig. 7.

Fig. 7 shows that the results calculated by the proposed method are more accurate. In order to further verify the accuracy of the proposed method, the mean harmonic voltage responsibilities and the relative calculation errors in the sampling time are computed, as shown in Table 2. Table 2 denotes

TABLE 3. Calculation results of three method.

Method	$ Z_s \cos \theta (\Omega)$		
	Low-voltage side	F1	F3
Method1	1.24	1.14	1.11
Method2	1.30	-0.63	0.90
Proposed method	1.48	1.29	1.25

Method	T_c (%)		
	Low-voltage side	F1	F3
Method1	29.92	17.02	13.61
Method2	31.36	-9.41	11.03
Proposed method	35.71	19.26	15.33

the relative error of the proposed method is 1.14%, and it is obviously smaller than that of the other two methods.

V. FIELD MEASUREMENT STUDIES

Field measurement studies are conducted based on the harmonic data of a 10kV bus in Machong 110kV transformer substation in Dongguan city, Guangdong province, China. The three-phase short-circuit capacity of the system is known as 333.76MVA, and the 10kV bus has 8 feeders, including specialized F1 and F3 for an industrial customer called Dongguan Glasses Company. The main power devices of this company are air compressors and water pumps, which are typical harmonic sources.

To determine the responsibilities of harmonic pollutions, the harmonic data are measured using a three-phase PQ analyzer device HIOKI PW3198, and the measuring locations and the sampling time are listed as follows:

- 1) The low-voltage side of the transformer substation, 2015.6.12 12:00~2015.6.13 06:00;
- 2) F1 feeder, 2015.6.8 12:00~2015.6.9 08:00;
- 3) F3 feeder, 2015.6.9 12:00~2015.6.10 10:00.

The device gives a set of measured amplitude data of the harmonic voltage and current per 3s. Taking the 5th harmonic as an example, all the collected harmonic data are shown in Fig. 8, and Fig. 9 shows the diagram of the substation. The three methods mentioned in Section IV are used to quantify the harmonic responsibilities at the three different locations, and the calculation results are given in Table 3. When we use the proposed method, the length of W is 1 min, one sliding window includes 20 sets of harmonic voltage and current amplitude data.

Based on the 5th harmonic power data collected by HIOKI PW3198 and the short-circuit capacity of the system, the equivalent harmonic impedances of the three measuring locations can be estimated to be 1.51Ω , 1.25Ω , and 1.21Ω , respectively. It can be seen from Table 3 that the harmonic voltage responsibility of all the 8 feeders is mainly assumed by F1 and F3, while the harmonic responsibilities of the remaining feeders are too low. The calculation results of method 1 are small, and method 2 is more effective if the measuring location is at the low-voltage side of the substation, and the calculation errors are large for the feeder measurement. Compared with method 1 and method 2, the calculation results of the proposed method are more accurate.

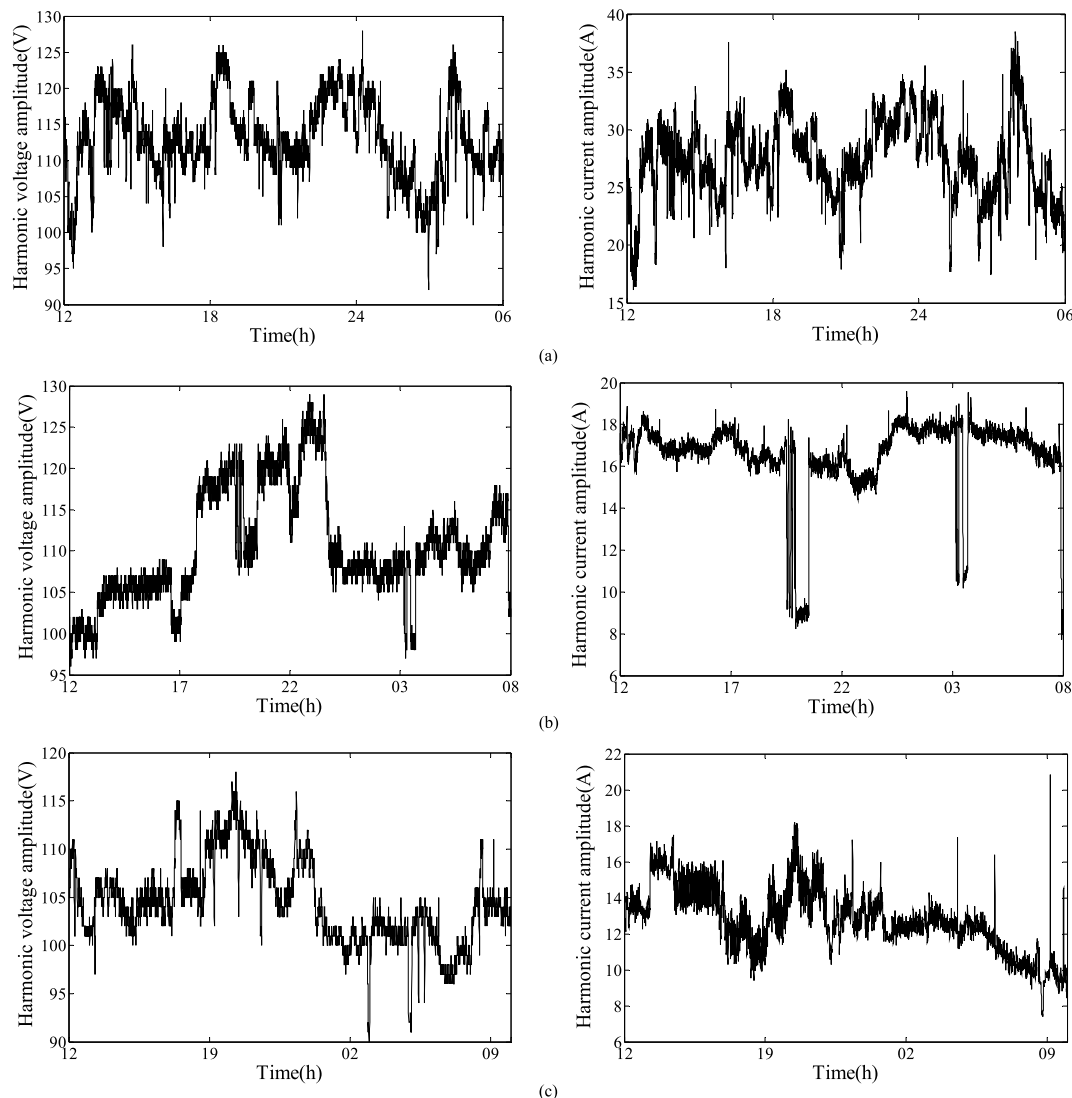


FIGURE 8. Waveforms of measured data. (a) The 5th harmonic data at the low-voltage side of the substation, (b) The 5th harmonic data of F1 feeder, (c) The 5th harmonic data of F3 feeder.

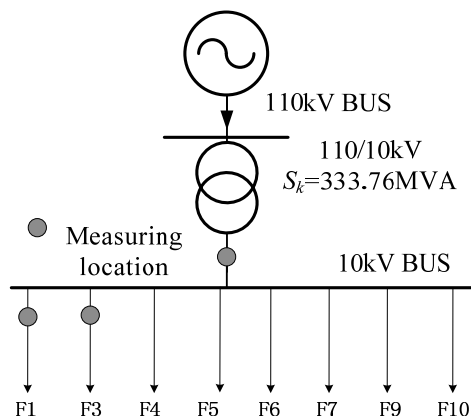


FIGURE 9. Diagram of machong substation.

VI. CONCLUSIONS

A novel harmonic responsibility quantification method is proposed in this paper based on the kurtosis detection principle

of the amplitude fluctuations. The proposed method extends traditional fluctuation method to the amplitude domain, and the data requirement can be met easily in actual projects. To ensure the accuracy of estimating the equivalent harmonic impedance, the kurtosis detection and interval estimate approaches are utilized to filter the measured data considering the synchronous fluctuations of the harmonic voltage and current, which reduces the influence of unstable background harmonics on the calculation results.

Simulation and field measurement studies show that the proposed method is applicable to the harmonic responsibility quantification regardless of the measuring location, and the calculation results are more accurate than those of the existing methods. The proposed method provides an effective help for analyzing the pollutions and traces of the harmonic sources.

Extended studies can be further carried out in the following aspects. First, the data pre-processing can be considered to avoid the abnormal data and improve the accuracy and

stability of the proposed method. Second, the reasonable selection of the window length can be further studied. Finally, the harmonic analysis under different operating modes can be conducted respectively considering the changes in the system operating modes.

REFERENCES

- [1] S. Bhattacharyya, S. Cobben, P. Ribeiro, and W. Kling, "Harmonic emission limits and responsibilities at a point of connection," *IET Gener., Transmiss. Distrib.*, vol. 6, no. 3, pp. 256–264, Mar. 2012.
- [2] J.-H. Han et al., "A new assessment for the total harmonic contributions at the point of common coupling," *J. Elect. Eng. Technol.*, vol. 9, no. 1, pp. 6–14, 2014.
- [3] H. E. Mazin, W. Xu, and B. Huang, "Determining the harmonic impacts of multiple harmonic-producing loads," *IEEE Trans. Power Del.*, vol. 26, no. 2, pp. 1187–1195, Apr. 2011.
- [4] W. Xu and Y. Liu, "A method for determining customer and utility harmonic contributions at the point of common coupling," *IEEE Trans. Power Del.*, vol. 15, no. 2, pp. 804–811, Apr. 2000.
- [5] F. Karimzadeh, S. Esmaili, and S. H. Hosseinian, "A novel method for noninvasive estimation of utility harmonic impedance based on complex independent component analysis," *IEEE Trans. Power Del.*, vol. 30, no. 4, pp. 1843–1852, Aug. 2015.
- [6] J. Hui, H. Yang, S. Lin, and M. Ye, "Assessing utility harmonic impedance based on the covariance characteristic of random vectors," *IEEE Trans. Power Del.*, vol. 25, no. 3, pp. 1778–1786, Jul. 2010.
- [7] F. M. Fernandez and P. S. C. Nair, "Method for separation of customer and utility contributions of harmonics at point of common coupling," *IET Gener. Transmiss. Distrib.*, vol. 7, no. 4, pp. 374–381, Apr. 2013.
- [8] W. Wang, E. E. Nino, and W. Xu, "Harmonic impedance measurement using a thyristor-controlled short circuit," *IET Gener., Transmiss. Distrib.*, vol. 1, no. 5, pp. 707–713, Sep. 2007.
- [9] M. Nagpal, W. Xu, and J. Sawada, "Harmonic impedance measurement using three-phase transients," *IEEE Trans. Power Del.*, vol. 13, no. 1, pp. 272–277, Jan. 1998.
- [10] J. Hui, W. Freitas, J. C. M. Vieira, H. Yang, and Y. Liu, "Utility harmonic impedance measurement based on data selection," *IEEE Trans. Power Del.*, vol. 27, no. 4, pp. 2193–2202, Oct. 2012.
- [11] W. Zhang and H.-G. Yang, "A method for assessing harmonic emission level based on binary linear regression," in *Proc. Int. Conf. CSEE*, 2004, pp. 50–54.
- [12] A. Zebardast and H. Mokhtari, "Technique for online tracking of a utility harmonic impedance using by synchronising the measured samples," *IET Gener. Transmiss. Distrib.*, vol. 10, no. 5, pp. 1240–1247, Jul. 2016.
- [13] T. Zang, Z. He, L. Fu, Y. Wang, and Q. Qian, "Adaptive method for harmonic contribution assessment based on hierarchical K-means clustering and Bayesian partial least squares regression," *IET Gener. Transmiss. Distrib.*, vol. 10, no. 13, pp. 3220–3227, Oct. 2016.
- [14] A. Zebardast and H. Mokhtari, "New method for assessing the utility harmonic impedance based on fuzzy logic," *IET Gener. Transmiss. Distrib.*, vol. 11, no. 10, pp. 2448–2456, Jul. 2017.
- [15] F. Karimzadeh, S. Esmaili, and S. H. Hosseinian, "Method for determining utility and consumer harmonic contributions based on complex independent component analysis," *IET Gener. Transmiss. Distrib.*, vol. 10, no. 2, pp. 526–534, Feb. 2016.
- [16] T. Pfajfar, B. Blazic, and I. Papic, "Harmonic contributions evaluation with the harmonic current vector method," *IEEE Trans. Power Del.*, vol. 23, no. 1, pp. 425–433, Jan. 2008.
- [17] H. Yang, P. Porotte, and A. Robert, "Assessing the harmonic emission level from one particular customer," in *Proc. 3rd Int. Conf. Power Qual.*, vol. 2, no. 8, pp. 160–166, 1994.
- [18] H. L. Gong, X. Y. Xiao, Y. M. Liu, and H. G. Yang, "A method for assessing customer harmonic emission level based on the dominant fluctuation filtering principle," *Proc. Chin. Soc. Elect. Eng.*, vol. 30, no. 4, pp. 22–27, 2010.
- [19] X. Zhao and H. G. Yang, "A new method to calculate the utility harmonic impedance based on FastICA," *IEEE Trans. Power Del.*, vol. 31, no. 1, pp. 381–388, Feb. 2016.
- [20] W. Xu, R. Bahry, H. E. Mazin, and T. Tayjasanant, "A method to determine the harmonic contributions of multiple loads," in *Proc. IEEE PES Gen. Meeting*, Calgary, AB, Canada, Jul. 2009, pp. 1–6.
- [21] M. Shojaie and H. Mokhtari, "A method for determination of harmonics responsibilities at the point of common coupling using data correlation analysis," *IET Gener. Transmiss. Distrib.*, vol. 8, no. 1, pp. 142–150, Jan. 2014.
- [22] E. O. de Matos, T. M. Soares, U. H. Bezerra, M. E. de Lima Tostes, A. R. A. Manito, and B. C. Costa, "Using linear and non-parametric regression models to describe the contribution of non-linear loads on the voltage harmonic distortions in the electrical grid," *IET Gener. Transmiss. Distrib.*, vol. 10, no. 3, pp. 1825–1832, May 2016.
- [23] J. Bai, W. Gu, X. Yuan, Q. Li, B. Chen, and X. Wang, "Power quality warning of high-speed rail based on multi-features similarity," *J. Elect. Eng. Technol.*, vol. 10, no. 1, pp. 92–101, 2015.
- [24] W. Gu, J. Bai, X. Yuan, S. Zhang, and Y. Wang, "Power quality early warning based on anomaly detection," *J. Elect. Eng. Technol.*, vol. 9, no. 4, pp. 1171–1181, 2014.
- [25] J. B. McDonald, J. Sorensen, and P. A. Turley, "Skewness and kurtosis properties of income distribution models," *Rev. Income Wealth*, vol. 59, no. 2, pp. 360–374, 2013.
- [26] J. Tian, C. Morillo, M. H. Azarian, and M. Pecht, "Motor bearing fault detection using spectral kurtosis-based feature extraction coupled with K-nearest neighbor distance analysis," *IEEE Trans. Ind. Electron.*, vol. 63, no. 3, pp. 1793–1803, Mar. 2016.
- [27] J. Bai, W. Gu, X. Yuan, Q. Li, F. Xue, and X. Wang, "Power quality prediction, early warning, and control for points of common coupling with wind farms," *Energies*, vol. 8, no. 9, pp. 9365–9382, 2015.
- [28] T. Qu et al., "Quality of electric energy supply-harmonic in public supply network," Standardization Admin. China, Beijing, China, Tech. Rep. GB/T 14549-93, 1993.

JIAN WU received the B.S. degree in electrical engineering from Hohai University, China, in 1996, and the M.S. degree in electrical engineering from North China Electric Power University, China, in 2015.

He is currently an Engineer with State Grid Suzhou Power Supply Company, Jiangsu, China. His research interests include power quality and active distribution networks analysis.

HAIFENG QIU (S'18) received the B.Eng. degree in electrical engineering from Nanjing Normal University, Nanjing, Jiangsu, China, in 2015.

He is currently pursuing the Ph.D. degree with the School of Electrical Engineering, Southeast University, Nanjing. His research interests include power quality, microgrid modeling, energy management, and optimization.

JINLONG XU is currently an Engineer with State Grid Suzhou Power Supply Company, Jiangsu, China. His research interests include power quality and distributed generations.

FEI ZHOU is currently an Engineer with State Grid Suzhou Power Supply Company, Jiangsu, China. His research interests include modeling and control of power systems and electric vehicles.

KANG DAI is currently an Engineer with State Grid Suzhou Power Supply Company, Jiangsu, China. His research interests include power system operation and planning.

CHEN YANG is currently an Engineer with State Grid Suzhou Power Supply Company, Jiangsu, China. His research interests include distributed control and optimization of power systems.

DONG LV is currently an Engineer with State Grid Suzhou Power Supply Company, Jiangsu, China. His research interests include power quality, smart meters, and smart homes.

...